

# Enthalpy Relaxation and Embrittlement of Poly(L-lactide) during Physical Aging

Pengju Pan, Bo Zhu, and Yoshio Inoue\*

Department of Biomolecular Engineering, Tokyo Institute of Technology, 4259-B-55 Nagatsuta, Midori-ku, Yokohama 226-8501, Japan

Received August 2, 2007; Revised Manuscript Received October 16, 2007

**ABSTRACT:** The enthalpy relaxation behavior of poly(L-lactide) (PLLA) below glass transition temperature ( $T_g$ ) and its effects on the mechanical properties were studied using differential scanning calorimetry (DSC), dynamic mechanical thermal analysis (DMTA), and tensile test. Both the enthalpy loss ( $\delta_H$ ) and peak endothermic temperature ( $T_p$ ) in the glass transition region show a linear increase with the logarithm of aging time ( $t_a$ ). On the basis of DSC results, the kinetics of the enthalpy relaxation process were analyzed, and the kinetic parameters of PLLA were obtained: relaxation rate of enthalpy at 40 °C  $\beta_H = 1.77 \text{ J g}^{-1}$  per decade, and apparent activation energy  $\Delta h^* = 1107 \text{ kJ mol}^{-1}$ . Besides, analysis on the kinetic of enthalpy relaxation for poly(DL-lactide) (PDLLA) shows that the  $\Delta h^*$  value of PDLLA is similar to that of PLLA. Moreover, it was found that the strength and modulus of PLLA increase gradually; on the contrary, the toughness reduces dramatically during the physical aging. The yield strength and tensile modulus increased respectively 18.8% and 23.1% after being aged at 40 °C for 1008 h, as compared to the unaged sample. Also, the fracture strain of PLLA decreased from more than 300% to about 6% with aging at 25 °C for 24 h. Moreover, the fractographic examination evaluated by scanning electron microscopy showed that the fracture of PLLA changed from the “ductile” to “inductile” manner during physical aging. The drop of ductility in physical aging is correlated to the rearrangement of polymer chains from disordered to more ordered morphology.

## Introduction

Poly(L-lactide) (PLLA), as a biodegradable polymer, has tremendous potential in both traditional and nontraditional applications where thermoplastics are employed. Since it degrades to nontoxic lactic acid, which is naturally present in the human body, PLLA can be used in implant materials, surgical suture, and controlled drug delivery systems. Furthermore, the attributes of biodegradability, producibility from renewable resources, good mechanical properties, and versatile fabrication processes make it a promising material for many disposable products, such as baby diapers and plastic bags as well as for traditional applications where common thermoplastics are employed, for instance, industrial devices, packaging, film, and fiber materials.<sup>1</sup>

The glass transition temperature ( $T_g$ ) of PLLA locates around 60 °C. When implanted or used in ambient conditions, the PLLA material will be at a temperature lower (but close) to the  $T_g$ . During the rapid cooling processing of PLLA, when it is cooled through its glass transition, molecular mobility slows down and the material becomes a thermodynamically unstable glass. From this nonequilibrium glassy state, the material system will tend to reach the equilibrium through the slow rearrangements. This phenomenon is often referred to as physical aging.<sup>2</sup> Physical aging can have a particularly profound impact on polymeric products during their service life, and it has been reported that many physical properties, such as mechanical properties, barrier resistance, optical properties, and crystallization behavior of amorphous polymers, are greatly affected by this aging process.<sup>3–10</sup> Consequently, the structural relaxation (or physical aging) in the glassy state is very important in determining the long-term performance of the material system. Owing to the influence of physical aging on physical properties of polymers,

in the past few decades, considerable attention has been awarded to investigate the physical aging behavior of polymers, such as polycarbonate, poly(ethylene terephthalate), polystyrene, polypropylene, and so on.<sup>3–10</sup>

Among the family of biomass-derived biodegradable polymers, PLLA has relatively high strength and modulus. Nevertheless, it is brittle and its fracture strain is only about 5% in the tensile test, which has been a major bottleneck for its large-scale commercial applications. Accordingly, development of the PLLA-based materials with high toughness has attracted wide attention in recent years.<sup>11</sup> The previous research suggested that the brittleness of PLLA is due to the low entanglement density ( $V_e$ ) and the high value of characteristic ratio ( $C_\infty$ ), a measure of chain stiffness.<sup>12</sup> Furthermore, it has been reported that the entanglement density of polymer chain changes during the physical aging process, which will induce the variation of mechanical properties, especially the toughness and fracture performance of polymers.<sup>2,3g,h</sup> Therefore, it is considered that the mechanical properties of PLLA are also dependent on the aging process. Thus, the study on the relationship between physical aging, morphology, and mechanical properties can probably provide some approaches to improve the toughness of PLLA-based materials.

In the present work, the effects of physical aging on the enthalpy relaxation, mechanical properties, and the fracture mechanism of PLLA were investigated by means of differential scanning calorimetry (DSC), dynamic mechanical thermal analysis (DMTA), and tensile test. The kinetics parameters of the aging process were evaluated on the basis of DSC analysis. Besides, the effect of physical aging on the mechanical properties was explained from the viewpoint of the rearrangement of polymer chains. For a comparison, the enthalpy relaxation behavior was also studied for poly(DL-lactide) (PDLLA).

\* To whom correspondence should be addressed: phone +81-45-924-5794. Fax: +81-45-924-5827. E-mail: inoue.y.af@m.titech.ac.jp.

## Experimental Section

**Materials.** The samples of PLLA ( $M_n = 121 \text{ kg mol}^{-1}$ ,  $M_w/M_n = 1.54$ ) and PDLA ( $M_n = 46 \text{ kg mol}^{-1}$ ,  $M_w/M_n = 1.91$ ; isotactic diad fraction  $[i] = 0.50$ ) were kindly supplied by Shimadzu Co. (Kyoto, Japan). The glass transition temperatures ( $T_g$ ) of PLLA and PDLA are about 58 and 45 °C, respectively, which were evaluated using DSC by heating the quenched samples at a heating rate of  $10 \text{ °C min}^{-1}$ . Before use, all the samples were purified by precipitating into ethanol from chloroform solution, and then they were dried in 40 °C vacuum oven for 3 days.

The dried PLLA and PDLA samples were placed on the Teflon sheets, sandwiched between the flat metal plates, and were hot-pressed after melted at 200 °C for 2 min. Then the pressed samples were quenched to  $23 \pm 0.5 \text{ °C}$ . The wide-angle X-ray diffraction (WAXD) measurements reveal that the PLLA samples prepared in this condition were amorphous due to the absence of any crystalline peak. The same processing conditions (temperature, time, and pressure) were maintained throughout to ensure reproducibility in the sample preparation. All the hot-pressed samples have a thickness of 0.38–0.40 mm.

**Measurements. Gel Permeation Chromatography (GPC).** Molecular weight of the PLLA and PDLA samples was measured on TOSOH HLC-8220 GPC system assembled with a VISCOTEK T-60AV viscometer. Chloroform was used as the eluent at a flow rate of  $1.0 \text{ mL min}^{-1}$ . TOSOH TSK standard polystyrene samples with the narrow molecular weight distribution were used as standards to calibrate the GPC elution curve.

**Differential Scanning Calorimeter (DSC).** The measurements of enthalpy relaxation were made using a Pyris Diamond DSC instrument (Perkin-Elmer Japan Co., Tokyo, Japan). The scales of temperature and heat flow at different heating rates were calibrated using an indium standard with nitrogen purging. Besides, daily baseline calibrations were performed at each heating rate to eliminate any baseline noise.

In the isothermal enthalpy relaxation experiments, samples which were to be annealed for times of 6 h or less were weighted and sealed in an aluminum pan, immediately after quenching, and they were annealed directly in the DSC. Because it is impractical to use the DSC as an oven for longer annealing times, for annealing times larger than 6 h, the samples were transferred, immediately after quenching, into an oven controlled at  $40 \pm 0.2 \text{ °C}$ . Following the annealing for certain time, the samples were quickly sealed in an aluminum pan for DSC measurement. In the DSC analysis, all the samples were scanned from 0 to 100 °C at  $10 \text{ °C min}^{-1}$ . No discontinuity was observed between the results obtained for the samples annealed for less than and greater than 6 h, indicating that the two annealing procedures (in the DSC and oven) are equivalent.

A further set of experiments was conducted to examine the effect of cooling rate on the enthalpy relaxation. In these experiments, the quenched PLLA and PDLA samples were initially held at 75 °C for 2 min to erase its thermal history. Then, they were cooled to 0 °C at various cooling rates, followed by a reheating from 0 to 100 °C at  $10 \text{ °C min}^{-1}$  immediately after the cooling stage.

**Dynamic Mechanical Thermal Analysis (DMTA).** The PLLA films, prepared as described above, were machined to the dimension required by DMTA measurement (30 mm  $\times$  10 mm) and tensile test (a gauge length of 22.25 mm and a gauge width of 4.76 mm), and then they were transferred to oven or refrigerator for aging. Before the measurement all the specimens were held at  $23 \pm 0.5 \text{ °C}$  for 10 min in order to erase the effect of temperature on the mechanical properties, and all the tests were conducted at this temperature.

The dynamic experiments were carried out in the tensile mode under atmospheric air using a DMS210 (Seiko Instrument, Japan) equipped with a SSC5300 controller. The frequency was chosen as 1 Hz, the heating rate as  $2 \text{ °C min}^{-1}$ , and the initial temperature as  $-10 \text{ °C}$ , which is controlled by the flow of liquid nitrogen.

**Tensile Test.** Tensile properties were measured with the help of Shimadzu (Tokyo, Japan) EZ test machine at a cross-head speed of  $2 \text{ mm min}^{-1}$ . Each value of mechanical properties reported was

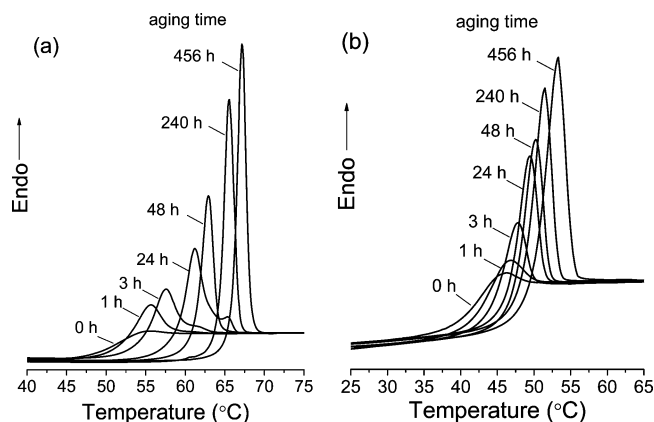


**Figure 1.** DSC curves on heating at  $10 \text{ °C min}^{-1}$  in the glass transition region for (a) PLLA and (b) PDLA samples annealed at 40 °C for the time (in hours) indicated on each curve.

an average of seven specimens. The Young's modulus  $E$  was obtained from the tangent of the initial slope of the stress vs strain curve.

**Scanning Electron Microscopy (SEM).** A scanning electron microscope (model JSM-5200, JEOL, Japan) was used to evaluate the morphology of fractured surfaces for the unaged and aged PLLA samples after the tensile test. The samples were sputter-coated with gold particles up to a thickness of about 10 nm before the surface characterization.

## Results and Discussion

**Effect of Aging Time on Enthalpy Relaxation.** DSC heating curves for PLLA samples annealed at 40 °C ( $\approx T_g - 18 \text{ °C}$ ) for the various times are shown in Figure 1a. The usual behavior of glassy polymers can be seen here. The area of the endothermic peak increases, and meanwhile the endothermic peak shifts to higher temperature with the increase of aging time ( $t_a$ ). When the polymer is quenched from the temperature above  $T_g$ , the polymer chains are frozen and their segmental mobility is drastically reduced. With aging of the material, the segmental mobility causes volume relaxation and thus reduction of the free volume, which has been experimentally confirmed by Cowie et al.<sup>10c</sup> Finally, the aged sample has smaller free volume as well as the smaller enthalpy and potential energy than the unaged one. Therefore, when the materials are reheated, more energy is required for the glass transition, resulting in the increase of the area of endothermic peak.<sup>3a</sup> Moreover, because of the reduction of segmental mobility, it is necessary to heat up to higher temperatures to finish the morphological rearrangement which occurred in the glass transition process. Accordingly,  $T_g$  is also increased during physical aging. Figure 1b presents the DSC heating scans of the PDLA samples annealed at 40 °C ( $\approx T_g - 5 \text{ °C}$ ) for different times. It can be seen that with increasing aging time the DSC curves of PDLA show the very similar variation trend as those of PLLA.

As shown in Figure 1a, as for PLLA, a shoulder is present at the high-temperature side of the main endothermic peak when  $t_a$  is between 3 and 24 h. However, this small shoulder is not detected for the aged PDLA samples, as shown in Figure 1b. This is possibly due to the existence of small amount of crystalline phase in the polymer, which is probably developed during the quenching process. Very recently, it has been reported that two endothermic peaks are present in the glass transition region of the heating DSC scans for the aged semicrystalline poly(ethylene terephthalate) and PLLA.<sup>5a,13</sup> It has been assigned that the lower temperature side peak corresponds to the

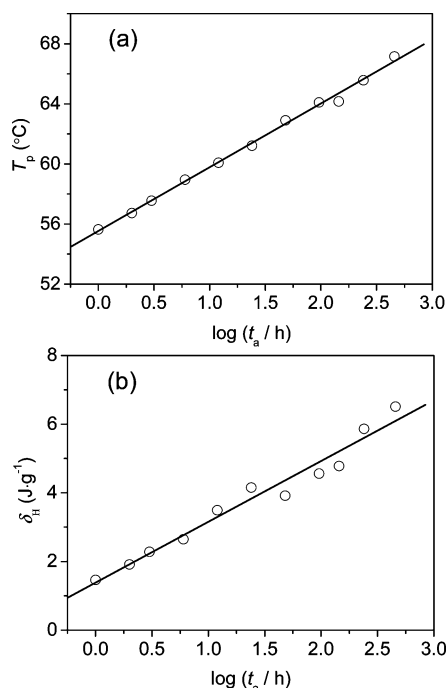


**Figure 2.** Dependence of (a) peak temperature ( $T_p$ ) and (b) enthalpy loss ( $\delta_H$ ) during physical aging of PLLA at 40 °C as a function of  $\log(\text{aging time}, t_a/h)$ . The full lines represent the linear least-square fit to the data.

segmental dynamics in the bulklike phase, and the higher temperature one is assigned to the constrained motion in the amorphous phase located within the crystalline phase. Here, the peak located at higher temperature-side is much smaller, as compared to the lower temperature one, indicating that the content of crystalline phase is extremely small.

On the basis of the DSC curves shown in Figure 1a, the temperature at the endothermic peak  $T_p$  and the enthalpy loss  $\delta_H$  (sometimes called “enthalpy recovered”) during annealing were obtained as a function of the aging time. The latter is found from the area difference between the DSC curves of the annealed samples and the reference unannealed sample. As for PLLA, the peak temperature and the enthalpy loss are plotted against the logarithm of aging time in parts a and b of Figure 2, respectively. As depicted in Figure 2, both the  $T_p$  and  $\delta_H$  values increase linearly with  $\log(t_a)$ , which is in well agreement with the results reported for polycarbonate.<sup>3a</sup> Although the PLLA and PDLLA samples were both aged at 40 °C in this isothermal annealing, the value of  $T_g - T_a$  for PDLLA ( $T_g - T_a \approx 5$  °C) is much smaller than that of PLLA ( $T_g - T_a \approx 18$  °C). Therefore, it is considered that the enthalpy relaxation kinetics of PLLA and PDLLA are possibly incommensurable. Here only the enthalpy relaxation kinetics of PLLA during isothermal annealing were analyzed.

The enthalpy recovered during physical aging depends on the thermal history that a glassy polymer experiences and on the related experimental variables, such as cooling rate  $q_1$ , annealing temperature  $T_a$ , annealing time  $t_a$ , and heating rate  $q_2$ . In this isothermal enthalpy relaxation experiments, all the variables except for  $t_a$  are fixed. Hence, it provides a direct measure of the overall relaxation rate of polymer segments. For instance, for a bulk sample, the relaxation rate  $\beta_H$ , which is a reasonable indicator of the aging kinetics, is usually defined as<sup>14</sup>

$$\beta_H = [\partial \delta_H / \partial (\log t_a)]_{q_1, q_2, T_a} \quad (1)$$

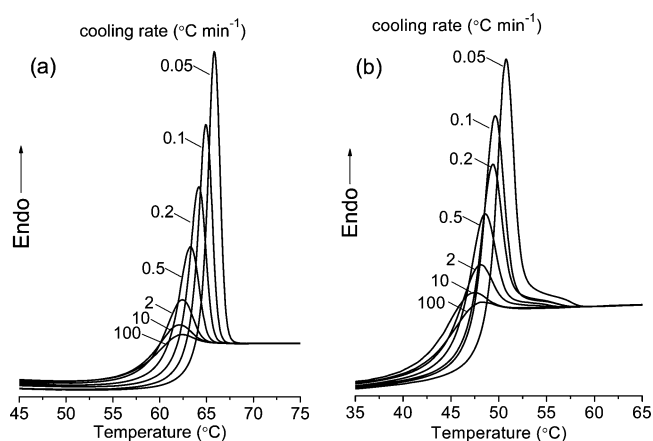


**Figure 3.** DSC heating scans at 10 °C min<sup>-1</sup> in the glass transition region for (a) PLLA and (b) PDLLA samples cooled at the various rates (in °C min<sup>-1</sup>) indicated on each curve.

where  $\beta_H$  can be estimated from the slope of enthalpy loss vs  $\log(t_a)$  plot. The slopes of the best fit straight lines in Figure 2a,b give the following values of  $T_p$  and  $\delta_H$  on  $\log(t_a)$  with  $T_a = 40$  °C,  $q_2 = 10$  °C min<sup>-1</sup>:  $\partial T_p / \partial (\log t_a) = 4.24$  °C per decade and  $\beta_H = \partial \delta_H / \partial (\log t_a) = 1.77$  J g<sup>-1</sup> per decade, with correlation coefficients of 0.998 and 0.983, respectively.

**Effect of Cooling Rate on Enthalpy Relaxation.** The effect of cooling rate on the enthalpy relaxation of PLLA was also investigated. The heating scans for PLLA samples cooled at the different rates are presented in Figure 3a. It can be seen that the glass transition behavior of PLLA is greatly dependent on the thermal history. With decreasing the cooling rate, the glass transition peak shifts to higher temperature, and both the intensity of endothermic peak and the  $T_g$  value increase. These imply that there are possibly some morphological differences among these samples developed at the various cooling rates.

This variation of polymer morphology during physical aging can be generally characterized in the terms of a limiting fictive temperature,  $T_f$ , as described by Ritland and Moynihan.<sup>15a,b</sup> This parameter is directly related to the state of aging for glassy materials.  $T_f$  of a material in a given state is defined as the temperature at which the equilibrium liquid has a relaxational value of  $p$  the same as that of the system in that state, where  $p$  is a macroscopic property of a vitreous system, such as, enthalpy, volume, and refractive index, etc.<sup>15a,b</sup> During the physical aging, the value of  $T_f$  will decrease in a manner that characterizes the relaxation kinetics. The  $T_f$  value can be directly evaluated from the original DSC heating curves.<sup>2b,3g,h,15b</sup> Figure 4 illustrates the determination of fictive temperature from the experimental enthalpy vs temperature data, which can be attained from the integration of DSC heat flow vs temperature curve. The  $T_f$  value can be determined as the intersection of the extrapolated pre-transition and post-transition baselines on this enthalpy vs temperature curve, as shown in Figure 4. The dependence of  $T_f$  on the cooling rate  $q_1$  can be written as<sup>3a,c,15</sup>

$$d(\ln|q_1|)/d(1/T_f) = -\Delta h^*/R \quad (2)$$

where  $\Delta h^*$  is the apparent activation energy for the enthalpy relaxation and  $R$  is the universal gas constant. The plot of  $\ln|q_1|$  vs reciprocal fictive temperature for PLLA is presented in Figure 5. A reasonably straight line was fitted to the data with a correlation coefficient of  $-0.996$ . From the slope, it was obtained that  $\Delta h^*/R = 133$  100 K, and hence the apparent activation energy  $\Delta h^* = 1107$  kJ mol<sup>-1</sup>. Besides, the enthalpy relaxation of PDLLA, which is intrinsically amorphous in nature,



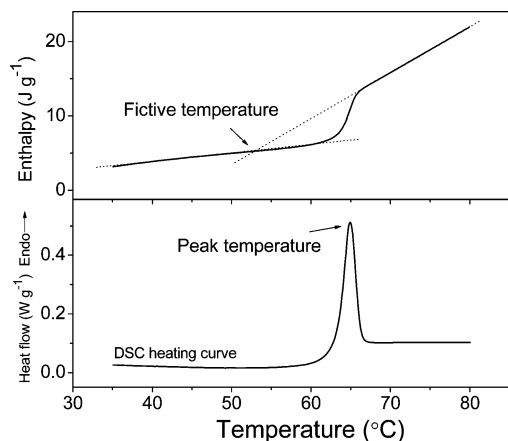


**Figure 4.** Schematic determination of fictive temperature from enthalpy vs temperature curve.

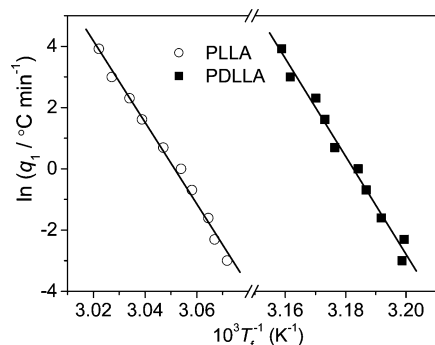


**Figure 5.** Plot of  $\log(\text{cooling rate}, q_1/^\circ\text{C min}^{-1})$  vs reciprocal fictive temperature ( $T_f$ ) of PLLA and PDLLA samples for the heating curves shown in Figure 3. The full lines represent the linear least-squares fit to the data.

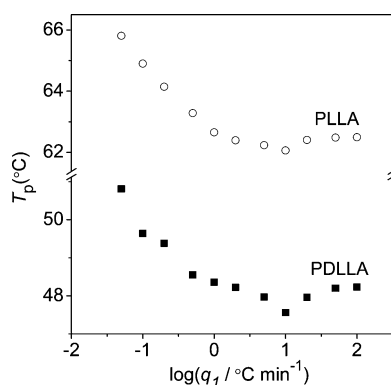


**Figure 6.** Dependence of peak temperature ( $T_p$ ) of PLLA and PDLLA samples on  $\log(\text{cooling rate}, q_1/^\circ\text{C min}^{-1})$  for the heating curves shown in Figure 3.

by cooling at different rates was also studied. As depicted in Figure 3b, as for PDLLA, the variation of DSC heating curves with the cooling rate shows a very similar tendency with that of PLLA. Moreover, the apparent activation energy for the enthalpy relaxation of PDLLA was also evaluated. According to eq 2, it was obtained that  $\Delta h^* = 1123 \text{ kJ mol}^{-1}$ .

On the basis of the results shown in Figure 3, the peak temperatures in the DSC curves of PLLA and PDLLA samples cooled at each rate are shown in Figure 6. Obviously, with decreasing the cooling rate, the peaks shift first to lower and then to higher temperatures when the cooling rate reduces below about  $10^\circ\text{C min}^{-1}$ . This phenomenon was also observed for polycarbonate.<sup>3a</sup> It has been proposed that this behavior represents a change in the nature of the endothermic peak from

an upper peak (invariant with annealing time) at the faster cooling rates, which gives poorly stabilized glasses with large values of excess enthalpy before reheating, to a main or annealing peak (strongly dependent on the annealing time) at the slower cooling rates, which gives increasingly well stabilized glasses with reduced values of excess enthalpy before reheating.<sup>3a</sup> In addition, it is also suggested that this reversal of the change in peak temperature is likely caused by the additional aging of the more quickly cooled samples on the subsequent slower heating.<sup>16</sup>

The activation energy  $\Delta h^*$  has been linked to the configurational energy barrier and reportedly reflects the cooperative nature of a relaxation process.<sup>17a</sup> Besides,  $\Delta h^*$  is greatly dependent on the structure and morphology of the polymer, and it has been found that increasing the cross-linking density as well as incorporation of nanoparticles in the polymer will induce the increase of  $\Delta h^*$  due to the restriction of segmental relaxation.<sup>14a,15c,17b</sup> The calculated  $\Delta h^*$  of PLLA ( $\Delta h^*/R = 133\,100 \text{ K}$ ) is a little smaller than that of polycarbonate reported by Hodge ( $\Delta h^*/R = 150\,000 \text{ K}$ ).<sup>3b</sup> This can be possibly explained by that the chain of polycarbonate bearing bisphenol A groups is more rigid than that of PLLA because the higher rigidity of polymer chain naturally requires a higher configurational activation threshold.<sup>17c</sup>

As evaluated previously, the  $\Delta h^*$  value of PDLLA is comparable with that of PLLA. Since the physical aging is accompanied by the rearrangement of polymer chains, besides the chemical structure, the configuration and conformation of polymer chains will also affect its relaxation behavior. The spectroscopic simulation performed by Hsu et al.<sup>18a</sup> indicated that the incorporation of the D unit into PLLA chains changes the chain conformation, particularly at the D–L junctions. Besides, the distribution of D and L units in the polymer chain also affects the chain conformation. So, the relaxation process of PDLLA will become more complicated as compared to that of PLLA. On the other hand, the kinetics parameters for the enthalpy relaxation process also depend on the molecular weight of polymer.<sup>18b</sup> Therefore, it is difficult to make a completely quantitative comparison between the relaxation mechanism of PDLLA and PLLA only from the  $\Delta h^*$  values.

**Dynamic Mechanical Thermal Analysis.** The temperature-dependent curves of storage modulus ( $E'$ ), loss modulus ( $E''$ ), and  $\tan \delta$  are presented in Figure 7a–c for unaged PLLA and PLLA aged at  $25^\circ\text{C}$  ( $\approx T_g - 33^\circ\text{C}$ ) for 96 and 480 h, respectively. The  $E'$ ,  $E''$ , and  $\tan \delta$  values for the three samples give almost the same curves above  $70^\circ\text{C}$ . An increase in the  $E'$  and  $E''$  curves appears between  $100$  and  $140^\circ\text{C}$ ; this is attributable to the cold crystallization occurring in this temperature range during heating.

However, significant difference among the PLLA samples with various heat histories is observed in the  $E'$ ,  $E''$ , and  $\tan \delta$  curves below  $T_g$ . As shown in Figure 7a, the  $E'$  value increases after aging. Besides, the temperature at the onset of the steep decrement of the  $E'$  curve for the aged samples is higher than that for the unaged sample (see inset in Figure 7a). As shown in Figure 7b,c, both the widths of the  $E''$  and  $\tan \delta$  peaks decrease with aging. In addition, corresponding well with the DSC results, the onset temperature of the glass transition peak in both the  $E''$  and  $\tan \delta$  curves increases with increasing  $t_a$ . These observations can be attributed to the decrease in the amount of free volume with aging, as suggested by the theory of Fox and Flory.<sup>19</sup> However, it can be discerned from Figure 7b,c that with the increase of aging time the temperature of glass transition peak is almost not changed, which is different

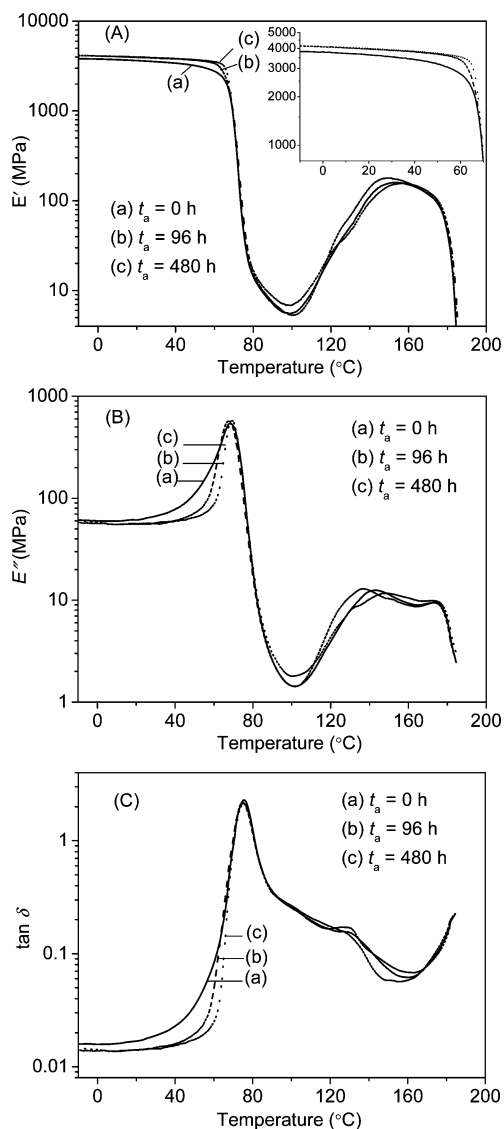


**Figure 7.** Temperature dependence of (A) storage modulus, (B) loss modulus, and (C)  $\tan \delta$  of (a) unaged PLLA and PLLA annealed at 25 °C for (b) 96 h and (c) 480 h.

from the previous DSC data. This is likely due to the interaction of this heating scan in DMTA measurement with the previous aging process. In other words, the morphology of the original sample can change during the heating process at a low heating rate of 2 °C min<sup>-1</sup>, especially at temperature close to the  $T_g$ .<sup>3e</sup>

**Tensile Test.** The tensile properties of the PLLA specimens unaged and aged at 4 °C ( $\approx T_g - 54$  °C), 25 °C, and 40 °C for various periods were investigated, and the stress–strain curves for the unaged samples and the samples annealed at 25 °C for 6 and 144 h are depicted in Figure 8. Clearly, the mechanical properties of PLLA are significantly dependent on the thermal history. The unaged PLLA specimen can elongate to 300% of its original length. Besides, the neck is formed during tensile deformation of the unaged sample, signifying that it is ductile and flexible. Nevertheless, as shown in Figure 8, there is a significant reduction in the fracture strain with increasing  $t_a$ , in parallel with the increase in yield strength and tensile modulus. The fracture strain, yield strength, and tensile modulus of PLLA samples aged at 25 °C for 144 h are 4.41%, 50.1 MPa, and 1509 MPa as compared to those of the unaged PLLA, 304%, 44.8 MPa, and 1323 MPa, respectively.

In order to analyze the fracture mechanism of the unaged and aged PLLA specimens, the morphology of the fracture

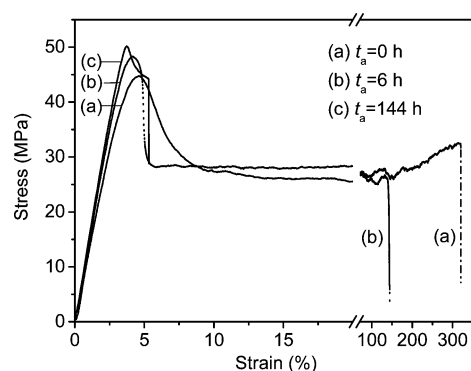


**Figure 8.** Tensile stress–strain curves of (a) unaged PLLA and PLLA aged at 25 °C for (b) 6 h and (c) 144 h.

surface was evaluated using SEM after the tensile test. The SEM micrographs of the unaged and aged (at 25 °C for 144 h) PLLA samples are shown in Figure 9. As shown in Figure 9a, as for the unaged PLLA specimen, the fracture surface is relatively regular, with the long ridges and valley relief which are parallel to the film plane and perpendicular to the stress direction. This observation is quite similar to the fracture surface of polycarbonate, which is characterized as a ductile material with high toughness.<sup>20a</sup> Besides, the fibrils of the oriented polymer, which are the remnants of crazes, can be observed in Figure 9a. These signify that the unaged PLLA is much more ductile, which undergoes the crazing and fibrillation process in the tensile deformation. The crazes, unlike cracks, are both a precursor to cracking and a toughening mechanism in stressed polymer. Crazing can be very beneficial because it is an energy-absorbing plastic-deformation process.<sup>20b</sup> All these indicate that the unaged sample has good deformation ability, and its fracture is in the “ductile” manner. However, the aged PLLA specimen fractures in a totally different way. As seen in Figure 9b, the surface is relatively flat and has lost its orderly ridges and valley relief. Moreover, large cracks or cavities are present in the surface, and their edges are also sharp. These indicate the failure of aged PLLA under tensile loadings is mainly in the “brittle” manner. This observation agrees well with the results reported by other authors.<sup>20c,d</sup> On the other hand, some microfibrils are also shown in Figure 9b, signifying that the PLLA specimen aged at 25 °C for 144 h still remains some features of plastic deformation.

The yield strength, tensile modulus, and fracture strain of PLLA samples annealed at 4, 25, and 40 °C were evaluated and plotted as a function of logarithm of aging time in parts a, b, and c of Figure 10, respectively. The wide-angle X-ray diffraction (WAXD) measurements show that the WAXD pattern of PLLA annealed at 40 °C for 1008 h is the same as that of quenched PLLA samples, and no diffraction peak is present, confirming that crystallization did not occur during this aging process. It can be seen that there is a significant increase in the yield strength and tensile modulus with increasing  $t_a$ . As for PLLA samples aged at 40 °C, the yield strength and tensile modulus approximately improved by 18.8% and 23.1% after aged for 1008 h, respectively, as compared to the unaged one. The aging time of 1008 h corresponds to 3.0035 in the logarithm scale shown in Figure 10. Also, in contrast to the unaged PLLA specimen, the yield strength and tensile modulus of those samples annealed at 25 °C for 1008 h increased by about 12.5% and 16.6%, respectively. Furthermore, as shown in Figure 10a,b, the increase of both yield strength and tensile modulus becomes more significant for PLLA samples aged for the same period, with the increase of the aging temperature.

Nevertheless, the variation of fracture strain of PLLA during physical aging is more complicated, as depicted in Figure 10c.

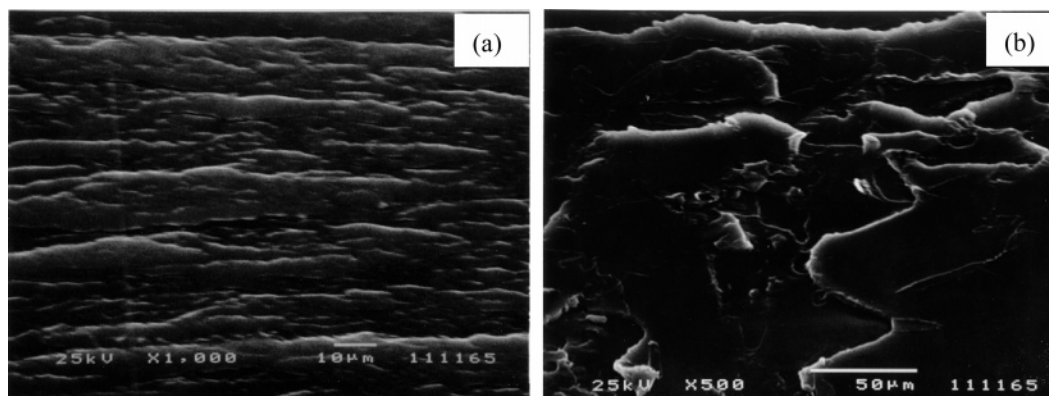


**Figure 9.** SEM of the fracture surface of (a) unaged and (b) aged (at 25 °C for 144 h) PLLA specimens.

As for the samples aged at 4 °C, the fracture strain decreased successively with increasing  $t_a$ . For the samples annealed at 25 °C, the fracture strain decreased from more than 300% to about 6% with aging for about 24 h, and it reduced gradually with increasing  $t_a$  when  $t_a$  is shorter than 24 h. The fracture strain is almost not changed for samples aged for a time longer than 24 h. However, with respect to the samples aged at 40 °C, the fracture strain reduced to about 6% suddenly after aged for only 1.5 h, and then it nearly did not vary with increasing  $t_a$ . This is probably due to the fact that the fracture strain is more sensitive to the ductility of the polymer than the yield strength and the tensile modulus.

**Morphological Variation during Physical Aging.** Since glassy polymers are in a nonequilibrium state after quenching, these materials will pursue a state closer to the equilibrium state due to the interactions of the polymer chains, which is usually accompanied by changes in physical properties. The inter- and intramolecular interaction between the polymer molecules can be outlined in a concept of the potential energy landscape.<sup>21</sup> This landscape, defined as a distribution of valleys (energy minima), mountains (energy maxima), and mountain pass (saddle point), is not static but is subject to dynamic processes dominated by vibrations and relaxation between local minima. These dynamic processes lead to local rearrangement of the chain segments and a slow loss of energy consequently.<sup>6a</sup>

During physical aging, the potential energy of the glassy polymer reduces and the minima become deeper. With the increase of aging temperature, the relaxation and rearrangement of polymer chains become quicker. Accordingly, the sample aged at higher temperature has a lower potential energy after aged for a certain period. In the tensile deformation, the polymer chains were orientated, and thus the free volume and potential energy are increased. Consequently, the relationship between the variation of potential energy ( $\Delta E$ ) in the tensile test, which is related to the required energy for establishing yielding, between the unaged and aged samples can be given as  $\Delta E(40\text{ °C}) > \Delta E(25\text{ °C}) > \Delta E(4\text{ °C}) > \Delta E(\text{unaged})$ , where  $\Delta E(40\text{ °C})$ ,  $\Delta E(25\text{ °C})$ , and  $\Delta E(4\text{ °C})$  represent the  $\Delta E$  of sample aged at 40, 25, and 4 °C for a certain period, respectively. Therefore, as shown in Figure 10a, the yield strength increases during aging, and it also increases with the increase of aging temperature despite the same aging time.

The local energy minimization which occurs during physical aging must be interrelated to the conformational rearrangements of polymer chains. It has been reported that changes occurring in polycarbonate during physical aging below  $T_g$  show shifts from trans-cis to more stable trans-trans conformations with increasing aging time.<sup>3d,4d</sup> The trans-trans conformations, allowing closer local packing of the polymer chains than the

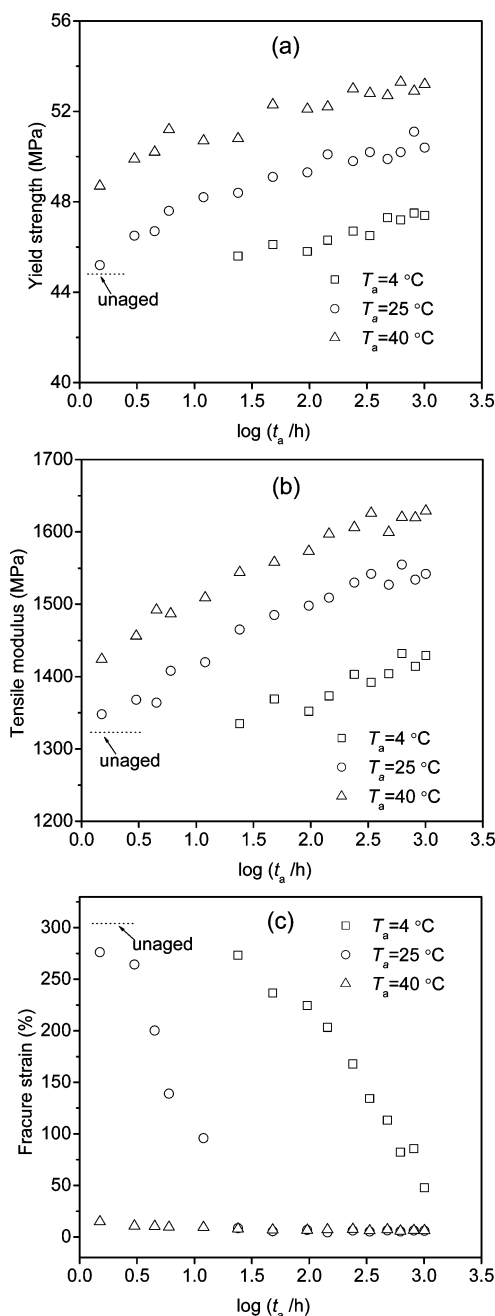


**Figure 10.** (a) Yield strength, (b) tensile modulus, and (c) fracture strain as a function of log(aging time,  $t_a$ /h) for PLLA samples annealed at 4, 25, and 40 °C. The dotted lines represent the data of the unaged PLLA specimen.



trans–cis ones, are also known to be more energetically stable. The similar conformational rearrangement has also been observed in the physical aging of poly(ethylene terephthalate) and polystyrene by means of FTIR spectroscopy.<sup>5b,e</sup> Previous studies showed that the amorphous PLLA mainly contains four distinct conformers, i.e., gt, gg, tg, and tt, in which the gt and gg conformers have the lowest and second lowest energy minimum.<sup>22</sup> Furthermore, the conformational populations change as the increase of temperature.<sup>22b</sup> Therefore, it is considered that the conformational changes are likely to take place in the amorphous PLLA during its physical aging. In other words, some gg, tg, and tt conformers seem to change into the most stable one, gt conformer, during the physical aging.

The drop of ductility in physical aging is correlated to the rearrangement of polymer chains in physical aging. As for polymer above  $T_g$ , owing to the larger free volume, the chains possess more mobility. Accordingly, the arrangement of polymer chains is more irregular and freer. In the quenching, the chains were frozen suddenly, and the morphology, which is similar to the one above  $T_g$ , was retained. Because of the more irregular arrangement of polymer chains, in the unaged PLLA some chains are possibly twisted and interlaced with each other. Therefore, the unaged PLLA is likely to possess a relatively disordered chains arrangement. During the aging process, because of the reduction of free volume,<sup>10c</sup> the polymer chains will rearrange from a loose packing of the quenched polymers toward more dense chain packing.<sup>7b</sup> Besides, recent studies by means of NMR, FTIR, and atomistic simulation suggested the presence of local order in physically aged polymer.<sup>4d,f</sup> So, it is reasonable to consider that the chain packing will become more and more ordered with physical aging. The unaged PLLA possesses larger free volume, and besides, the local strain can be more efficiently transferred through the more disorderly arranged polymer chains under tensile deformation. Accordingly, the unaged sample shows higher toughness and flexibility, as compared to the aged one. Besides, owing to the decreased mobility of polymer chains and less efficient transfer of local strain in the aged sample, the modulus of PLLA increases with increasing  $t_a$ .

## Conclusion

On the basis of the DSC analysis, the kinetics parameters of physical aging process for amorphous PLLA were evaluated. Amorphous PLLA has an apparent activation energy  $\Delta h^* = 1107 \text{ kJ mol}^{-1}$ , which is smaller than that of polycarbonate, indicating that the enthalpy relaxation of PLLA is easier and faster. Moreover, PLLA shows the similar  $\Delta h^*$  value to that of PLLA. The dynamic mechanical properties as well as the tensile properties of amorphous PLLA are quite dependent on the aging temperature and aging time. The yield strength and tensile modulus increase with the increase of aging time or aging temperature. Besides, the fracture strain decreases significantly during the physical aging, due to the drop of ductility and toughness.

The variation of ductility of PLLA during physical aging is correlated with the rearrangement of polymer chains. The more disordered polymer chains in unaged PLLA is more efficient for the transfer of local strain during mechanical deformation. Therefore, it is suggested that depressing the PLLA chain relaxation below  $T_g$  by means of cross-linking the polymer chains, synthesis of branched PLLA-based polymer, or incorporation of layered nanofiller, etc., is possibly the potential methods for improving the toughness of PLLA-based materials. Our future work will focus on the conformational behavior of

PLLA during its physical aging, which is of fundamental importance to elucidate the mechanism for chain rearrangement and to explain the dependence of mechanical properties on the aging process.

**Acknowledgment.** Bo Zhu gratefully acknowledges Japan Society for the Promotion of Science for providing the fellowship and the grant-in-aid to do this research at Tokyo Institute of Technology.

## References and Notes

- (1) (a) Aou, K.; Hsu, S. L. *Macromolecules* **2006**, *39*, 3337. (b) Jain, R. A. *Biomaterials* **2000**, *21*, 2475. (c) Ikada, Y.; Tsuji, H. *Macromol. Rapid Commun.* **2000**, *21*, 117.
- (2) (a) Hutchinson, J. M. *Prog. Polym. Sci.* **1995**, *20*, 703. (b) Hodge, I. M. *J. Non-Cryst. Solids* **1994**, *169*, 211. (c) Chen, K.; Schweizer, K. S. *Phys. Rev. Lett.* **2007**, *98*, 167802.
- (3) (a) Hutchinson, J. M.; Smith, S.; Horne, B.; Gourlay, G. M. *Macromolecules* **1999**, *32*, 5046. (b) Hodge, I. M. *Macromolecules* **1983**, *16*, 898. (c) Kovacs, A. J.; Hutchinson, J. M.; Ramos, A. R. *J. Polym. Sci., Polym. Phys. Ed.* **1979**, *17*, 1097. (d) Soloukhin, V. A.; Brokken-Zijp, J. C. M.; Van Asselen, O. L. J.; De With, G. *Macromolecules* **2003**, *36*, 7585. (e) Laot, C. M.; Marand, E.; Schmittmann, B.; Zia, R. K. P. *Macromolecules* **2003**, *36*, 8673. (f) Hodge, I. M. *Macromolecules* **1983**, *16*, 371. (g) Ho, C. H.; Vu-khanh, T. *Theor. Appl. Fract. Mech.* **2004**, *41*, 103. (h) Ho, C. H.; Vu-khanh, T. *Theor. Appl. Fract. Mech.* **2003**, *39*, 107.
- (4) (a) Robertson, C. G.; Wilkes, G. L. *Macromolecules* **2000**, *33*, 3954. (b) Shelby, M. D.; Hill, A. J.; Burgar, M. I.; Wilkes, G. L. *J. Polym. Sci., Polym. Phys.* **2001**, *39*, 32. (c) Araki, O.; Horie, M.; Masuda, T. *J. Polym. Sci., Polym. Phys.* **2001**, *39*, 337. (d) Dybal, J.; Schmidt, P.; Baldrian, J.; Kratochvil, J. *Macromolecules* **1998**, *31*, 6611. (e) Cangialosi, D.; Schut, H.; van Veen, A.; Picken, S. J. *Macromolecules* **2003**, *36*, 142. (f) Utz, M.; Atallah, A. S.; Robyr, P.; Widmann, A. H.; Ernst, R. R.; Suter, U. W. *Macromolecules* **1999**, *32*, 6191.
- (5) (a) Zhao, J.; Wang, J.; Li, C.; Fan, Q. *Macromolecules* **2002**, *35*, 3097. (b) Qian, R.; Shen, D.; Sun, F.; Wu, L. *Macromol. Chem. Phys.* **1996**, *197*, 1485. (c) Lu, X.; Hay, J. N. *Polymer* **2000**, *41*, 7427. (d) McGonigle, E. A.; Daly, J. H.; Gallagher, S.; Jenkins, S. D.; Liggat, J. J.; Olsson, I.; Pethrick, R. A. *Polymer* **1999**, *40*, 4977. (e) Magonov, S. N.; Shen, D.; Qian, R. *Macromol. Chem. Phys.* **1989**, *190*, 2563.
- (6) (a) Van Melick, H. G. H.; Govaert, L. E.; Raas, B.; Nauta, W. J.; Meijer, H. E. H. *Polymer* **2003**, *44*, 1171. (b) Wypych, A.; Duval, E.; Boiteux, G.; Ulanski, J.; David, L.; Seytre, G.; Mermet, A.; Stevenson, I.; Kozanecki, M.; Okrasa, L. *J. Non-Cryst. Solids* **2005**, *351*, 2593. (c) Kawana, S.; Jones, R. A. L. *Eur. Phys. J. E* **2003**, *10*, 223. (d) Thureau, C. T.; Ediger, M. D. *J. Chem. Phys.* **2002**, *116*, 9089.
- (7) (a) Cerrada, M. L.; McKenna, G. B. *Macromolecules* **2000**, *33*, 3065. (b) Tan, S.; Su, A.; Luo, J.; Zhou, E.; Cheng, S. Z. D. *Macromol. Chem. Phys.* **1999**, *200*, 2487.
- (8) (a) Wang, Y.; Mano, J. F. *J. Appl. Polym. Sci.* **2006**, *100*, 2628. (b) Cai, H.; Dave, V.; Gross, R. A.; McCarthy, S. P. *J. Polym. Sci., Polym. Phys. Ed.* **1996**, *34*, 2701. (c) Liao, K.; Quan, D.; Lu, Z. *Eur. Polym. J.* **2002**, *38*, 157. (d) Celli, A.; Scandola, M. *Polymer* **1992**, *33*, 2699.
- (9) (a) Huang, Y.; Paul, D. R. *Macromolecules* **2005**, *38*, 10148. (b) Huang, Y.; Paul, D. R. *Macromolecules* **2006**, *39*, 1554. (c) Huang, Y.; Paul, D. R. *Polymer* **2004**, *45*, 8377. (d) Krishnaswamy, R. K.; Geibel, J. F.; Lewis, B. J. *Macromolecules* **2003**, *36*, 2907.
- (10) (a) Andreozzi, L.; Faetti, M.; Giordano, M.; Zulli, F. *Macromolecules* **2005**, *38*, 6056. (b) Andreozzi, L.; Faetti, M.; Giordano, M.; Palazzuoli, D. *Macromolecules* **2002**, *35*, 9049. (c) Cowie, J. M. G.; Harris, S.; McEwen, I. J. *Macromolecules* **1998**, *31*, 2611. (d) Wypych, A.; Duval, E.; Boiteux, G.; Ulanski, J.; David, L.; Mermet, A. *Polymer* **2005**, *46*, 12523. (e) Priestley, R. D.; Ellison, C. J.; Broadbelt, L. J.; Torkelson, J. M. *Science* **2005**, *309*, 456.
- (11) (a) Shibata, M.; Inoue, Y.; Miyoshi, M. *Polymer* **2006**, *47*, 3557. (b) Kai, W.; Zhao, L.; Zhu, B.; Inoue, Y. *Macromol. Rapid Commun.* **2006**, *27*, 109.
- (12) (a) Tonelli, A. E.; Flory, P. J. *Macromolecules* **1969**, *2*, 225. (b) Joiasse, C. A. P.; Veenstra, H.; Grijpma, D. W.; Pennings, A. J. *Macromol. Chem. Phys.* **1996**, *197*, 2219. (c) Grijpma, D. W.; Penning, J. P.; Pennings, A. J. *Colloid Polym. Sci.* **1994**, *271*, 1068.
- (13) Wang, Y.; Gómez Ribelles, J. L.; Salmerón Sánchez, M.; Mano, J. F. *Macromolecules* **2005**, *38*, 4712.
- (14) (a) Lu, H.; Nutt, S. *Macromolecules* **2003**, *36*, 4010. (b) Struik, L. C. E. *Polymer* **1987**, *28*, 1869. (c) Bartos, J.; Muller, J.; Wendorf, J. H. *Polymer* **1990**, *31*, 1678.

- (15) (a) Ritland, H. N. *J. Am. Ceram. Soc.* **1954**, 37, 370. (b) Moynihan, C. T.; Easteal, A. J.; Debolt, M. A.; Tucker, J. *J. Am. Ceram. Soc.* **1976**, 59, 12. (c) Lu, H.; Nutt, S. *Macromol. Chem. Phys.* **2003**, 204, 1832.
- (16) Pyda, M.; Wunderlich, B. *Macromolecules* **2005**, 38, 10472.
- (17) (a) Karasz, F. E.; MacKnight, W. J. *Macromolecules* **1968**, 1, 537. (b) Rittigstein, P.; Priestley, R. D.; Broadbelt, L. J.; Torkelson, J. M. *Nat. Mater.* **2007**, 6, 278. (c) Cheng, S. Z. D.; Heberer, D. P.; Janimak, J. J.; Lien, S. H. S.; Harris, F. W. *Polymer* **1991**, 32, 2053.
- (18) (a) Kang, S.; Zhang, G.; Aou, K.; Hsu, S. L.; Stidham, H. D.; Yang, X. *J. Chem. Phys.* **2003**, 118, 3430. (b) Andreozzi, L.; Faetti, M.; Giordano, M.; Zulli, F. *Macromolecules* **2005**, 38, 6056.
- (19) Fox, T. G.; Flory, P. J. *J. Appl. Phys.* **1950**, 21, 581.
- (20) (a) Liu, K.; Piggott, M. R. *Polym. Eng. Sci.* **1998**, 38, 69. (b) Suresh, S. *Fatigue of Materials*, 2nd ed.; Cambridge University Press: Cambridge, 1998. (c) Li, Y.; Shimizu, H. *Macromol. Biosci.* **2007**, 7, 921. (d) Bhardwaj, R.; Mohanty, A. K. *Biomacromolecules* **2007**, 8, 2476.
- (21) Malandro, D. L.; Lacks, D. J. *J. Chem. Phys.* **1999**, 110, 4593.
- (22) (a) Kang, S.; Hsu, S. L.; Stidham, H. D.; Smith, P. B.; Leugers, M. A.; Yang, X. *Macromolecules* **2001**, 34, 4542. (b) Meaurio, E.; Zuza, E.; López-Rodríguez, N.; Sarasua, J. R. *J. Phys. Chem. B* **2006**, 110, 5790.

MA071737C